Novel Silicon/Aluminum (Si/Al) Alloys for use as Cold Plate Materials in Cryogenically Cooled Solid-State Lasers

John F. Schill[a], Andrew J.W. Ogilvy[b]
[a] U.S. Army Research Laboratory, 2800 Powder Mill Rd., Adelphi, MD 20783
[b]Sandvik Osprey Ltd., Sandvik Materials Technology, Millards, Neath SA11 1NJ, UK

Abstract

The issue of heat transfer in high energy lasers has been a serious problem for years. One valid method of mitigating this problem is the use of low quantum defect solid-state materials operated at cryogenic temperatures[1]. A significant problem exists due to mismatch of coefficient of thermal expansion (CTE) and repeatedly cycling through a temperature range of ~200 K. Other groups, T.Y. Fan et al at MIT Lincoln Laboratory, have used ingenious crystal holders to overcome this problem. In this paper, we suggest the use of silicon/aluminum (Si/Al) alloys produced by Sandvik Osprey Ltd. that can have their CTE altered easily to match the CTE of whatever crystal material is chosen and still have a thermal transfer coefficient suitable for large heat transfer. We show the results of testing three different Si/Al alloys for CTE and thermal conductivity. We further test the material in a flow boil-off cryogenic cooling system that shows that the CE6 alloy material is capable of heat transfer of 21.5KW/m^{2}K , with cold plate temperatures maintained below 110 K. The CE6 material has a CTE that almost exactly matches YAG from 90--300K.

1. Introduction

Over the past several years much work has been done towards development of a high power solid-state laser. Many groups have explored the use of cryogenic cooling in order to enhance the material properties at those temperatures. Higher thermal conductivity, lower thermal expansion, and lower thermo optic coefficient (dn/dT) than at room temperature lead to very attractive candidates for scalable high power solid state lasers. Many solid state materials exhibit improved spectroscopic properties at cryogenic temperatures that support high laser efficiency. For example, Yb:YAG at 100K becomes a four-level system with decreased saturation intensity and a quantum defect of only 9% [2].

One of the major problems encountered in these systems is the mismatch of CTE between the solid-state material and the heat sink. Often the solid-state material is soldered to the heat sink with indium (In), and repeated cycling between 100 K and 300 K weakens that connection. Being able to match the CTE and still maintain a high thermal conductivity into the heat sink is quite beneficial.

2. Alloy Material

Sandvik-Osprey Si/Al alloys are in growing demand for a variety of applications in electronics and allied industries. These alloys are available in the composition range 87% Si-13% Al to 12 %Si-88 %Al, which enables the coefficient of thermal expansion to be adjusted between 2.0 and 20 ppm/K (see Figure 1) so as to be compatible with many common microelectronic devices, substrates, and solid-state laser materials. An alloy of 87% Si-13% Al composition has been developed that exhibits a CTE of 2 ppm/K at 100K.

These alloys are typically between three and six times lighter than established packaging and baseplate materials used in RF and microwave products such as Kovar®, copper-molybdenum and copper-tungsten. At the same time, the Osprey CE Alloys offer greatly superior thermal conductivity compared to Kovar® a vital requirement for meeting the increased power loading requirements of the latest generation of devices and associated circuitry. They possess high specific stiffness, but are not unduly hard, and so are amenable to standard machining operations, such as milling and drilling, and are as easy to machine by EDM as Al. Machining operations do not produce burrs on the

higher silicon CE Alloy parts, in contrast with most other metals, and this obviates the need for operations to remove them. CE Alloys are readily platable, using industry proven methods. Being composed of Si and Al, the alloys are environmentally friendly, safe to handle and use, and present no disposal problems. As they do not contain strategic metals, such as cobalt (Co), tungsten (W), or molybdenum (Mo), CE Alloys are far less susceptible to price volatility and supply shortages. For example, the price of Mo has increased by a factor of ten since the beginning of 2004.

Their unusual combination of high thermal conductivity and low thermal capacity makes for easier soldering of solid-state materials and feedthroughs, as heat is distributed more evenly in CE alloy assemblies [Private communication, Thunderline Z, USA]. Because Al and Si are light metals, soldered regions, comprising heavy metals, are readily revealed by X-rays, greatly facilitating non-destructive inspection of joints.

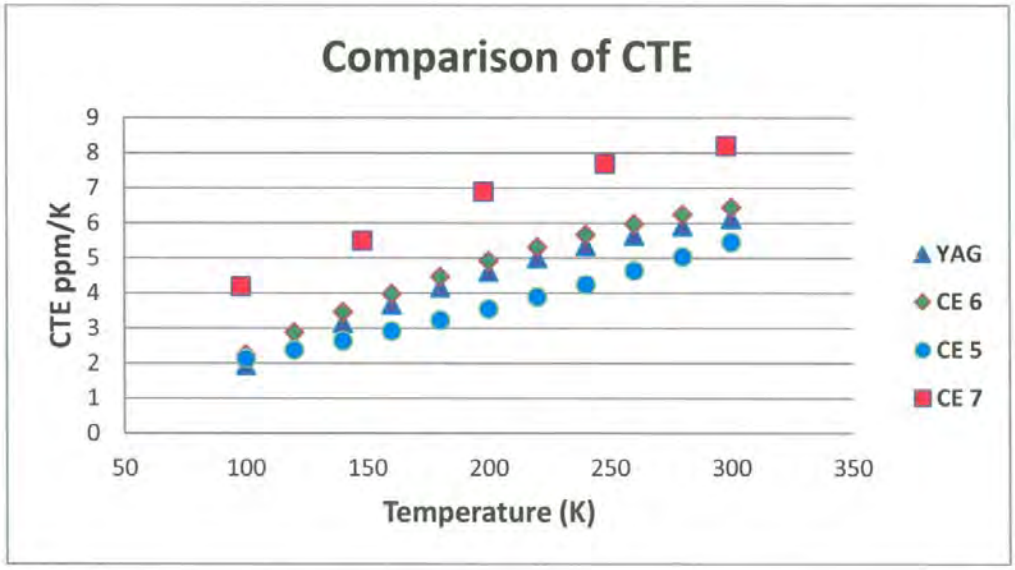

Figure 1. Graph of the CTE of several Si/Al alloys along with data for YAG[3]. This demonstrates how CTE can be tailored to the particular material chosen for the laser. Data collected at PMIC, Corvallis, OR except YAG[3]

In addition to their ability to match the CTE of most laser materials Si/Al alloys also exhibit high thermal conductivity. Figure 2. shows the thermal conductivity of several alloys. This testing was done at NETZSCH Instruments North America, LLC Burlington, MA. Note that the thermal conductivity of CE5 and CE6 are about 140 W/mK at 100K and that CE7 tends toward 330 W/mK if the trend of the data is extrapolated. As a comparison the thermal conductivity of YAG is about 47 W/mK[2] at 100K.

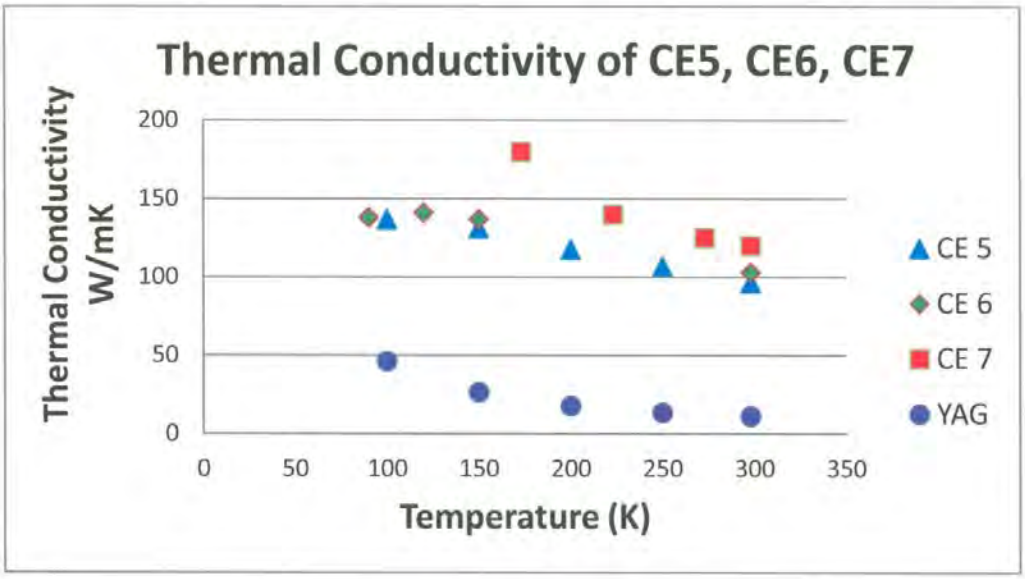

Figure 2. Thermal conductivity of several Si/Al alloys.

3. Flow Boiling

3.1 Introduction

Of the three main methods of cryogenic cooling, pool boiling, flow boiling, and evaporative spray cooling, forced convection flow boiling has the most promise. Pool boiling is the most limited because its heat handling capabilities are limited. Once the nucleate boiling regime has been passed, at approximately $\Delta T_{SAT} = 20$ K[4], the system is no longer able to control the temperature ($\Delta T_{SAT} = T_W - T_{BULK}$, temperature at the wall, temperature in the bulk liquid). On the other hand, in a flow boiling system, all one needs to do is increase the flow rate to compensate for the increased energy flow. Evaporative spray cooling is, in fact, a more efficient method of cryogenic cooling, but it requires complex spray systems.

3.2 Theory of Flow Boiling Heat Transfer

Analysis of flow boiling and its regimes can be very complex, especially when turbulent flows are encountered. Over the years, most of the correlations that have been postulated to describe the heat transfer characteristics are based on mathematical analysis of data compiled by many researchers. Each of the correlations has merit, but it seems that they often address a particular configuration and do not apply in general.

The regimes start with the least complex, forced convection due to laminar flow over the surface to be cooled, and proceed through dry-out, where there is so much heat that all the liquid is converted to vapor while it flows through the system. In-between, where our interest lies, there is nucleation and bubbly flow, plug flow where bubbles begin to join together, slug flow where there are large vapor gaps, wavy flow, stratified flow, and annular flow where the center of the flow region is vapor, while the walls have a film of vapor.

The primary mechanism for heat transfer in forced convection flow boiling is bulk turbulent transport[5]. In this regime, both liquid and vapor bubbles are flowing together in a non-laminar turbulent—with many eddy currents—way. The creation of vapor bubbles along the wall is the primary method of heat removal. Both phases are flowing together, and the rate of flow and the quality of the vapor are the important quantities. The Martinelli parameter (Equation 1) describes the vapor quality of the flow. The Reynolds Number (Equation 2) describes the flow rate.

$$X_{tt} = \left(\frac{1-x}{x}\right)^{0.9} \left(\frac{\rho_v}{\rho_l}\right)^{0.5} \left(\frac{\mu_l}{\mu_v}\right)^{0.1} \quad (1)$$

$$\mathrm{Re}_l = \frac{G(1-x)D_h}{\mu_l} \quad (2)$$

Here, x represents the fraction of the liquid that has been converted to vapor, ρ is the density in kg/m^3, μ is the viscosity in kg/m s, G is the mass flux in kg/m^2 s, and D is the characteristic length. In this case, the subscript h is added to denote the hydraulic diameter = 4 A/P, or four times the area of the duct over the perimeter. The subscripts v and l denote vapor and liquid respectively. Presently, we will need one other dimensionless number, the Prandlt number, Pr = $\mu C_p/k$, where C_p is the specific heat in J/kg K and k is the thermal conductivity in W/m K.

Over 60 years ago, Lockhart and Martinelli[6] postulated that two phase flows could be treated as separate superimposed flows in the same channel. Over the years many correlations have been developed in order to improve upon their correlation. The most cited correlation in the literature is the Chen correlation[7]. In this correlation, the two-phase heat transfer coefficient is given by.

$$h_{2\varphi} = E\, h_l + S h_b \quad (3)$$

Here, h_l is the liquid heat transfer coefficient and E is an enhancement factor, and h_b is the nucleate boiling or pool boiling heat transfer coefficient with S as a suppression factor. The single phase liquid heat transfer coefficient can be derived from the Dittus-Bolter equation[8] for turbulent flow (Equation 4),

$$h_l = 0.023\left(\frac{k_l}{D_h}\right) \mathrm{Re}_l^{0.8} \mathrm{Pr}_l^{0.4} \quad (4)$$

The pool boiling heat transfer coefficient can be evaluated using the Rohsenow equation[9], and the enhancement and suppression factors are given using the Martinelli parameter and the two-phase Reynolds number, as follows:

$$E = 1 \quad for \quad X_{tt}^{-1} \leq 0.1 \quad (5)$$

$$E = 2.35\left(0.213 + \frac{1}{x_{\mathrm{tt}}}\right)^{0.736} \quad for \quad X_{tt} > 0.1 \quad (6)$$

$$S = \left(1 + 2.56\, x\, 10^{-6}\, \mathrm{Re}_{2\varphi}^{1.17}\right)^{-1} \quad (7)$$

$$\mathrm{Re}_{2\varphi} = \mathrm{Re}_l (E)^{1.25} \quad (8)$$

$$q''_{nucleate} = \mu_l h_{fg} \left(\frac{g(\rho_l - \rho_v)}{\sigma}\right)^{0.5} \left(\frac{C_{pl(T_w - T_{sat})}}{C_{sf} h_{fg} \mathrm{Pr}_l^n}\right)^3 \quad (9)$$

Equation 9 is the Rohsenow equation[9] yielding the energy flux from pool boiling in W/m^2. Here, h_{fg} is the enthalpy of vaporization, σ is the surface tension of the liquid-vapor interface, T_w is the temperature of the wall, T_{sat} is the temperature of the bulk liquid far away from the wall or the saturation temperature of the liquid, and C_{sf} is a factor that represents the surface quality of the wall. This factor can make a significant difference because surface roughness will enhance the nucleation of the liquid and thereby increase the energy transfer into the liquid[9].

4. Experimental Setup

4.1 Physical Layout

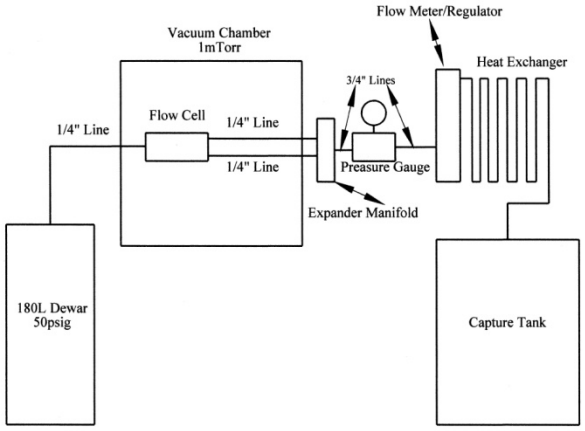

Figure 3. A schematic of the experimental set up.

Figure 3 is an overall schematic of the setup. We use a 180-L dewar of liquid nitrogen (LN_2) that is self pressurized to 50 psig. This pressure is the driving force that pushes the LN_2 through the system. The LN_2 is delivered to a rectangular duct of cross-sectional area $0.00048387m^2$ and length of .0381m via a one quarter- in. line, and it leaves the cell via two one quarter- in. lines. This is done to reduce the effect of increased pressure in the cell on the ultimate temperature of the sample due to increased saturation temperature. The cell is in a vacuum chamber that is maintained at about 1 mTorr. At the output of the chamber is a pressure gauge and a flow meter that will allow us to know the mass flux in the cell. A heater is applied to the line after the flow meter to vaporize any residual LN_2 before it reaches the collection tank.

Figures 4 and 5 are representations of the cold plate side of the cell and the side view looking perpendicular to the flow direction. In these views, you see the placement of the CE6 and the nine 200-W heaters that are soldered to the CE6 with indium (In). The CE6 is also soldered to the cell with In. The side view shows more clearly the placement of the thermocouples on the top and bottom of the CE6 and near the inner wall of the cell. These thermocouples are held in place with thermal epoxy. The electrical leads were soldered to the heaters using a 50/50 lead /tin alloy so that its melting temperature is higher than that of indium. This allows them to hold during the soldering of the CE6 and heaters.

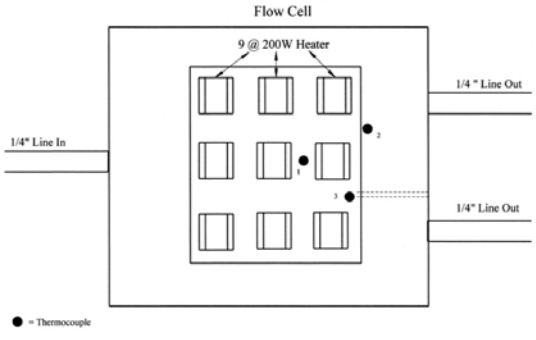

Figure 4. A view of the cell from below with CE6 and heaters.

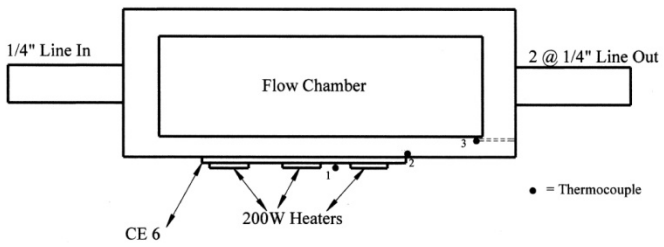

Figure 5. A view of the cell from the side showing the actual orientation of the CE6 and thermocouples.

5. Data

The data was collected over a number of weeks as we made improvements on the system. Table 1- is a representation of several runs made after the improvements were made and is repeatable. What is interesting to note is that the system was able to dissipate 121.4kW/m^2, with only a 6K increase in wall temperature. This same data reveals a heat transfer coefficient of 20.23kW/m^2K. There was additional data taken beyond this point, but there the system was no longer able to hold the wall temperature to a reasonable level, and the heat transfer coefficient went down significantly.

Table 1. Data that is representative of results taken over several days.

Current (A)	Voltage (V)	Power (W)	Sensor #1 (K)	Sensor #2 (K)	ΔT CE6 (K)	Sensor #3 (K)	Increase in wall Temperature
0	0	0	77	77	0	77	0
6	14.6	87.6	82.5	80.3	2.2	78.3	1.3
8	19.8	158.4	87.6	83.9	3.9	79.4	2.4
10	24.7	247	91.6	86.2	5.4	79.7	2.7
12	29.7	356.4	101.1	91.6	9.5	81	4
14	34.6	484.4	105.3	93.7	11.6	82.3	5.3
15	37.2	558	109.2	95.7	13.5	82.9	5.9

In addition to this experiment, we also ran an experiment in a similar setup with only one heater and a CE6 sample that was 15 mm x 10 mm. This test was able to verify the results from the independent test lab that show the thermal conductivity to be 140 W/mK at 100 K.

In addition to this data, some additional facts are needed to make an analysis of the data. Based on the flow measurement made in the system it was determined that the mass flux G= 272kg/m^2 s. Based on a mass flow of .1314kg/s and a heat of vaporization for LN_2 at 77K of 199.3KJ/kg, the vapor fraction at 550W into the system is 0.02.

6. Analysis

Based on the previous data, we can now calculate the two-phase heat transfer coefficient from the equations given in section 3 and the data from section 5. Using equation 2 and the hydraulic diameter of 0.016 m, G = 272kg/m^{2}s, x = 0.02, and μ_l= 158μPa-s @ 77K, we calculate a Re_l = 26,993. This Reynolds number indicates that we are well out of the transition region and into the turbulent region. The equations given should yield good results. From equation 4 and the Prandlt number taken from a table in[10], we can calculate the liquid heat transfer coefficient h_l = 11,435. From equation 1, we calculate X_{tt} = 3.5 and the enhancement factor equation 6 is 1.41. The two-phase Reynolds number given by equation 8 is calculated using the enhancement factor to yield 41,474. $Re_{2\varphi}$ is then used to calculate the suppression factor equation 7 S = 0.6071. We finally come to the Rohsenow equation (equation 9), where we will derive the heat transfer due to pool boiling. As mentioned earlier, the surface condition of the inner wall is very important in determining heat flux because roughness enhances nucleation sites. We used .0364 for C_{sf}. This number was derived from data taken by Nguyen et al[4], where the number was chosen to fit the data. With this and the fact that we had a ΔT_{sat} = 6K, we can find h_b = 1945. And finally using equation 3 we have $h_{2\varphi}$ = 17.3 kW/m^{2}K. This is in agreement with the data, with an error of 14.5%. This error is in very good agreement with the error bars many other groups get using various correlations. A good example of this is in a paper by Jackson et al[11] at the University of Florida.

7. Conclusion

We performed an experiment using a method of forced convection flow boil-off cooling. We found that our results were in good agreement with a theoretical analysis. Our analysis indicates that the contribution to the heat transfer coefficient from forced convection is more than 13 times greater than that from pool boiling. Other work that we have done at the U.S. Army Research Laboratory indicates that evaporative spray cooling is a more efficient method of cooling than flow boiling, but it is still unclear how much the spray systems can be scaled to handle higher powers. The flow boil-off system is well understood, and scaling will not be a problem. The limitation will come from the laser material because its heat transfer capabilities are very limited.

8. Acknowledgements

The authors would like to thank Mark Dubinskiy of the U.S. Army Research Laboratory (ARL) for his support both financial and technical during this work. We would also like to thank Nikoley Ter-Gabrielyan and Viktor Fromzel, also of ARL, for our many conversations regarding laser materials at cryogenic temperatures and the detrimental effects of thermal lensing in solid state lasers.

REFERENCES

[1] Ter-Gabrielyan, N., Merkle, L.D., Ikesae, A., Dubinskii, M., "Ultralow quantum-defect eye-safe Er:Sc_2O_3 laser," Optics Letters 33(13), 1524-1526 (2008).

[2] Ripin, D., Ochoa, J., Aggarwal, R., Fan, T.Y., "165-W Cryogenically Cooled Yb:YAG Laser," Optics Letters 29(18) , 2154-2156 (2004).

[3] Aggarwal, J., Ripin, D., Ochoa, J., Fan, T.Y., "Measurement of thermo-optic properties of $Y_3Al_5O_{12}$, Lu_3 Al_5O_{12}, $YAIO_3$, $LiYF_4$, $LiLuF_4$, BaY_2F_8, $KGd(WO_4)_2$, and $KY(WO_4)_2$ laser crystals in the 80–300 K temperature range," J. Appl. Phys. 98, 103514 (2005).

[4] Nguyen, D., Chen, R., Chow, L., Gu, C., "Effects of Heater Orientation and Confinement on Liquid Nitrogen Pool Boiling," J. of Thermophysics and Heat Transfer 14(1), 109-111 (2000).

[5] Dengler, C. E., and Addoms, J. N., "Heat Transfer Mechanism for Vaporization of Water in a Vertical Tube," Chemical Engineering Progress Symposium Series 52(18), 95-103 (1956).

[6] Chen, J. C., "Correlation for Boiling Heat Transfer to Saturated Fluids in Convective Flow," I&EC Process Design and Development 5(3), 322-329 (1966).

[7] Lockhart, R.W., Martinelli, R.C., "Proposed Correlation of Data for Isothermal Two Phase Flow, Two Component Flow in Pipes," Chem. Eng. Prog. 45, 39–48 (1949).

[8] Dittus, F. W., and Boelter, L. M. K., "Heat Transfer in Automobile Radiators of the Tubular Type," Publications in Engineering 2, 443 (1930).

[9] Rohsenlow, W. M., [Developments in Heat Transfer], The M.I.T. Press, Cambridge, 203-214 (1964).

[10] Barron, R.F., [Cryogenic Heat Transfer], Taylor and Frances, Philadelphia, 359 (1999).

[11] Jackson, J., Liao, J., Klausner, J.F., Mei, R., "Transient Heat Transfer During Cryogenic Chilldown," Proc. ASME HT2005 Conference, HT2005-72145, 90-91 (2005).